01 Jan 1979

Backscatter Inversion in Spherically Asymmetric Ionosphere

R. (Richard) E. DuBroff
Missouri University of Science and Technology, red@mst.edu

N. Narayana Rao

K. C. Yeh

Recommended Citation

R. E. DuBroff et al., "Backscatter Inversion in Spherically Asymmetric Ionosphere," *Radio Science*, vol. 14, no. 5, pp. 837 - 841, Wiley; American Geophysical Union, Jan 1979.
The definitive version is available at https://doi.org/10.1029/RS014i005p00837

Radio Science, Volume 14, Number 5, pages 837–841, September–October 1979

Backscatter inversion in spherically asymmetric ionosphere

R. E. DuBroff,[1] *N. Narayana Rao, and K. C. Yeh*

Department of Electrical Engineering, University of Illinois at Urbana-Champaign, Urbana, Illinois 61801

(Received July 17, 1978.)

It is well known that various diurnal and morphological features of the ionosphere reveal substantial departures from the normally simplified assumption of spherical symmetry at certain times of the day or at certain geographic locations. A radio ray passing through such an ionosphere must bear information about its horizontal gradients. The leading edge of a backscatter ionogram is formed by obliquely propagated radio rays of minimum time delay and hence is useful in deducing information about the ionospheric horizontal gradients. In this regard, the ionospheric electron density distribution is modeled by a locally quasi-parabolic layer with six parameters. This six-parameter space is known as the 'ionostate.' Our object is to seek the 'best' ionostate in the sense that the corresponding mean square error in group delay is a minimum. A computer program has been written to carry out the specified procedure. A number of sample calculations are presented and discussed.

1. INTRODUCTION

The problem of determining gross ionospheric structure from the analysis of various types of ionogram measurements has received increasing attention in recent years. The present work will be concerned entirely with the backscatter ionogram technique as discussed by *Croft* [1972]. Previous methods, as exemplified by *Rao* [1974, 1975] and *Hatfield* [1970], have utilized this technique in order to determine the parameters associated with a spherically symmetric model of the ionosphere. An approach recently suggested by *Chuang and Yeh* [1977] and based upon an adaptation of the teleseismic techniques discussed by *Backus and Gilbert* [1967] allows a more general determination of the ionospheric structure.

In contrast, the present work is directed toward the analysis of backscatter leading edges under conditions which allow for the absence of spherical symmetry. Formally, the method of solution is similar to the method used by *Rao* [1974].

2. METHOD OF SOLUTION

In order to generalize the earlier methods the quasi-parabolic electron density model used by *Rao* [1974, 1975] has been replaced by a locally quasi-parabolic electron density model in which the quasi-parabolic parameters may be assumed to vary with the angular displacement θ away from the backscatter sounder, i.e.,

$$N_e(r,\theta) = N_m(\theta)\left[1 - \left(\frac{r - r_m(\theta)}{r_m(\theta) - r_b(\theta)}\right)^2 \left(\frac{r_b(\theta)}{r}\right)^2\right] \quad (1)$$

where

$N_m(\theta)$ maximum value of electron density;
$r_m(\theta)$ geocentric distance to peak density;
$r_b(\theta)$ geocentric distance to base of ionosphere;
$N_e(r,\theta)$ electron density.

The two-dimensional representation of electron density is sufficient when it is assumed that the ray paths used to represent the backscatter signal are contained in a single azimuthal plane. This condition is satisfied for the present model by ignoring magnetoionic effects. For the particular case of linear gradients in all three quasi-parabolic parameters the phase refractive index n may be represented as

$$n(r,\theta,f,\tilde{\xi}) = \{1 - [(\xi_3 + \theta\cdot\xi_6)^2/f^2] \cdot [1 - [(r - \xi_2 - \theta\cdot\xi_5)^2(\xi_1 + \theta\cdot\xi_4)^2]/r^2 \cdot [\xi_2 + \theta\cdot\xi_5 - \xi_1 - \theta\cdot\xi_4]^2]\}^{1/2} \quad (2)$$

where f is the backscatter sounding frequency and

$$r_b(\theta) \equiv \xi_1 + \theta\cdot\xi_4$$

$$r_m(\theta) \equiv \xi_2 + \theta\cdot\xi_5$$

[1] Now at Phillips Petroleum Company, Bartlesville, Oklahoma 74004.

0048-6604/79/0910-0837$01.00

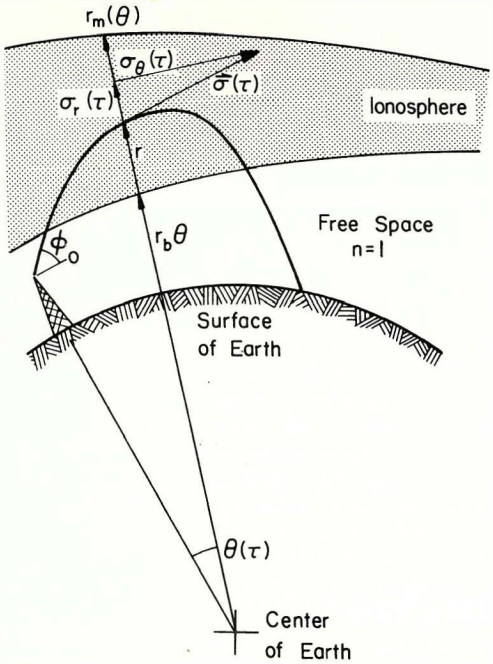

Fig. 1. Ray tracing geometry.

$$f_c(\theta) = \sqrt{80.6N_m(\theta)} \equiv \xi_3 + \theta \cdot \xi_6$$

thereby allowing the ionosphere model to be conveniently represented by a six-dimensional vector $\vec{\xi}$, whose first three components are the base radius, the peak radius, and the critical frequency, respectively, and the next three components are their respective spherical gradients.

At this point the problem becomes one of determining $\vec{\xi}$ based upon the observed backscatter leading edge. In this regard, the observed backscatter leading edge will be denoted by $\hat{P}'(f)$. In a similar manner, $\hat{P}'(f,\vec{\xi})$ will be used to denote the backscatter leading edge which would be measured if the ionosphere corresponded, in fact, to a locally quasi-parabolic electron density model specified by $\vec{\xi}$. The minimum group path along the backscatter leading edge may, in turn, be found through the solution of the ray equations.

The ray equations, as formulated for spherical coordinates by *Haselgrove* [1957], may be reduced to the present case by neglecting magnetoionic effects and the consequent azimuthal deviation of the rays. Following the notation of *Yeh and Liu* [1972], these equations may then be written as

$$\frac{dr}{d\tau} = \frac{\sigma_r}{n^2} \tag{3}$$

$$\frac{d\theta}{d\tau} = \frac{\sigma_\theta}{rn^2} \tag{4}$$

$$\frac{d\sigma_r}{d\tau} = \frac{1}{n}\frac{\partial n}{\partial r} + \sigma_\theta \frac{d\theta}{d\tau} = \frac{1}{n}\frac{\partial n}{\partial r} + \frac{\sigma_\theta^2}{rn^2} \tag{5}$$

$$\frac{d\sigma_\theta}{d\tau} = \frac{1}{rn}\frac{\partial n}{\partial \theta} - \frac{\sigma_\theta}{r}\frac{dr}{d\tau} = \frac{1}{rn}\frac{\partial n}{\partial \theta} - \frac{\sigma_\theta \sigma_r}{rn^2} \tag{6}$$

with the respective phase and group paths given by

$$dP/d\tau = 1 \tag{7}$$

$$dP'/d\tau = 1/n^2 \tag{8}$$

and with $\vec{\sigma}$ equal to the product of the phase refractive index n and the unit vector $\hat{k}$ in the wave normal direction.

Referring to Figure 1, the appropriate initial conditions, denoted by $\tau = 0$, can be seen to be

$$r(0) = \text{radius of the earth} = 6370 \text{ km} \tag{9}$$

$$\theta(0) = 0 \tag{10}$$

$$\sigma_r(0) = \sin\phi_0 \tag{11}$$

$$\sigma_\theta(0) = \cos\phi_0 \tag{12}$$

$$P(0) = P'(0) = 0 \tag{13}$$

The initial condition, in the form of ϕ_0, may then be varied in order to obtain the minimum group path for a given frequency. Assuming that the minimum group paths are thus computed for a

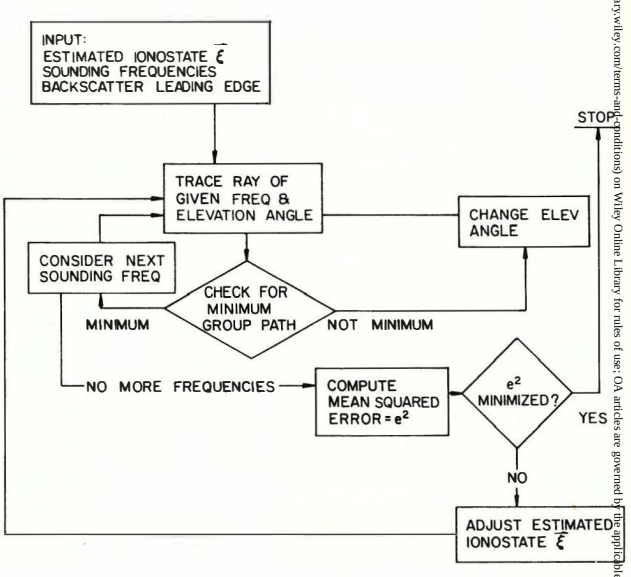

Fig. 2. Inversion program flow chart.

number N of discrete sounding frequencies f_i, a mean squared error e^2 may be computed according to

$$e^2(\vec{\xi}) = \frac{1}{N}\sum_{i=1}^{N} [\hat{P}'(f_i) - \hat{P}'(f_i, \vec{\xi})]^2 \qquad (14)$$

thereby defining a hypersurface over the domain of $\vec{\xi}$. Consequently, the present procedure consists of an initial estimate for $\vec{\xi}$ which is then adjusted in order to reduce the mean squared error. This procedure is summarized in Figure 2 and has been incorporated in a computer program.

While the detailed mechanics of the program are not germane to the present discussion, there are a few features which merit elaboration. The solution of the ray equations (i.e., (3)–(8)) is accomplished through the use of a common fourth-order Runge Kutta scheme [*Phillips and Taylor*, 1973] with an externally specified step size in τ. The adjustment of $\vec{\xi}$ in accordance with the minimization of e^2 utilizes a modified steepest descent technique. In addition, there is an external provision for distinguishing between fixed and variable components of $\vec{\xi}$. The fixed components are intended to remain unaltered throughout the procedure, while the variable components define the domain over which the minimization may be accomplished.

As a means of demonstrating this procedure and providing a reference ionosphere with known properties, simulation rather than direct measurement will be used to generate a backscatter leading edge, $\hat{P}'(f_i)$, which would be observed, in a locally quasi-parabolic model ionosphere corresponding to $\vec{\xi} = \vec{\xi}_0$. Various components of $\vec{\xi}_0$ will then be altered and the value of $\vec{\xi}$ thereby obtained, together with the backscatter leading edge $\hat{P}'(f_i)$, will act as input for the procedure shown in Figure 2.

3. RESULTS

With these provisions in mind, the simplest case is to assume that all except one of the components of $\vec{\xi}$ are fixed. The variable component in this case was chosen to be ξ_6 in order to demonstrate the capability of this procedure to determine the variation of one of the ionospheric parameters (i.e., critical frequency) with distance from the sounder. A simulation run was then used to determine the minimum group path (at 7 MHz) for a model ionosphere with $\vec{\xi} = [6570, 6720, 5, 0, 0, 2]$, and it was found that the minimum group path equaled

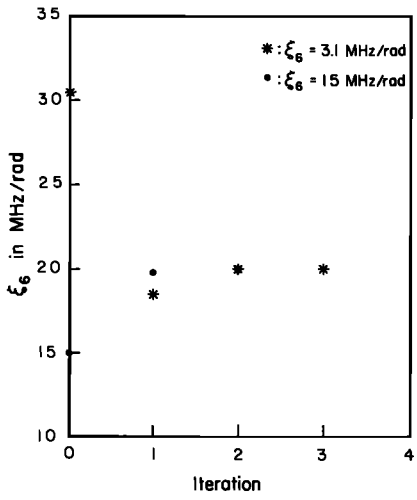

Fig. 3. Convergence of ξ_6 to its correct value. The correct value for ξ_6 is 2 MHz/rad. The dot corresponds to an initial trial value of 1.5 MHz/rad and the star to 3.1 MHz/rad.

1165.3 km. $\vec{\xi}$ was then set to [6570, 6720, 5, 0, 0, 1], thereby resulting in a different value of minimum group path at 7 MHz. The mean squared error (based on a single frequency in this case) was, in fact, found to be 14 km^2. However, when the value of ξ_6 was adjusted in accordance with the scheme shown in Figure 2, ξ_6 converged rapidly

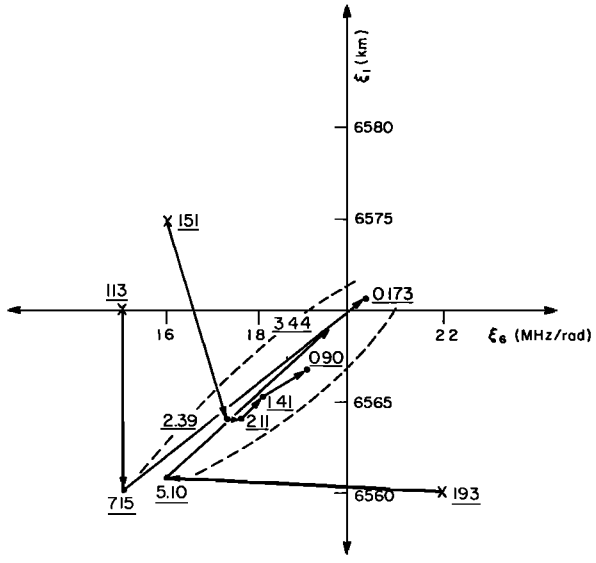

Fig. 4. Two-component (ξ_6 and ξ_1) convergence in the sense of least mean square error (MSE) defined by equation (14). The correct values correspond to the intersection of ξ_1 and ξ_6 axes. The starting values are marked by crosses. The underlined values are mean square errors in square kilometers.

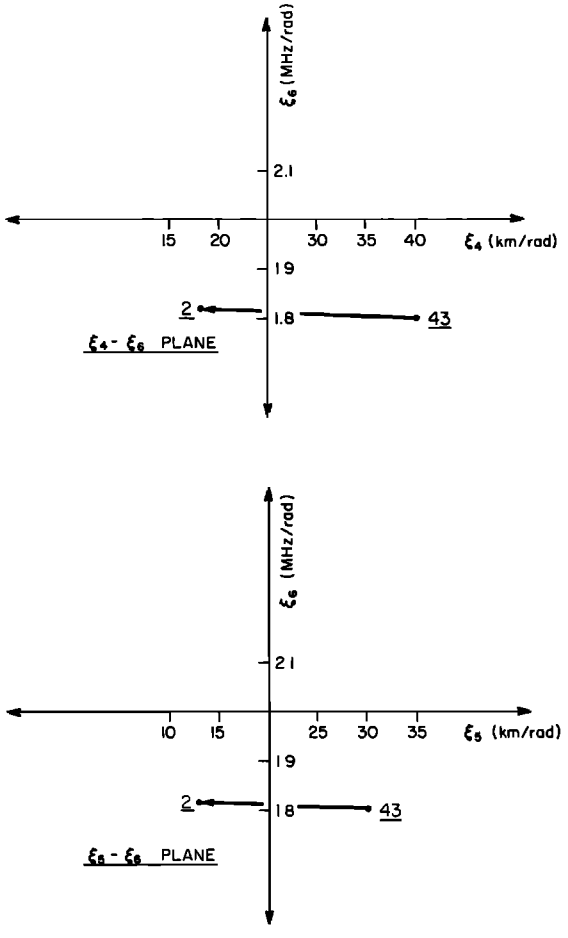

Fig. 5. Three-component (ξ_4, ξ_5, ξ_6) convergence of MSE.

to the correct value, and the mean squared error, of course, became negligible. This result is shown in Figure 3. A similar case is also shown for a starting value of $\xi_6 = 3.1$.

A more interesting demonstration of this procedure can be seen in Figure 4. In this case both ξ_1 and ξ_6 were allowed to vary from their initial values, which are indicated by the crosses in Figure 4. The correct values of ξ_1 and ξ_6 were, as before, 6570 km and 2 MHz/radian.

The underlined numbers in this figure are the values of the mean squared error (based upon two sounding frequencies) which were found to occur at various points along the trajectory in the ξ_1–ξ_6 plane. The dotted curves represent a portion of the contour line along which the mean squared error was found to be 7 km^2. Thus the convergence of ξ_1 and ξ_6 may be seen to have occurred primarily in a long and narrow valley in the mean squared error surface.

While the two cases which have already been discussed illustrate the determination of the critical frequency gradient (ξ_6), the case of three simultaneous gradients (i.e., a gradient in the critical frequency, a gradient in the base radius, and a gradient in the peak radius) has also been considered. In this case an ionosphere model of $\vec{\xi}$ = [6570, 6720, 5, 25, 20, 2] was used to simulate the measurement of a backscatter ionogram at three sounding frequencies. ξ_4, ξ_5, and ξ_6 were then specified as variable components. In Figure 5 it may be seen that the initial value of $\vec{\xi}$ was set equal to [6570, 6720, 5, 40, 30, 1.8]. The upper and lower sets of coordinate axes are used to represent the three-dimensional trajectory of ξ_4, ξ_5, and ξ_6 as projected upon two orthogonal planes. It can be seen that the mean squared error was reduced rapidly from an initial value of 43 km^2 to a value of 2 km^2. Additional results, which are not shown in Figure 5, have suggested that the convergence of the mean squared error is considerably slower as the mean squared error becomes smaller. This observation will be discussed in the following section.

4. CONCLUSION

Generally, the procedure seems to converge most rapidly when the mean squared error is large. A possible explanation of this observation is that the amount of 'noise' generated by the approximations used in this procedure (especially the Runge Kutta integration) becomes increasingly important as the mean squared error becomes smaller. Specifically, if it is assumed that the noise contributes approximately 0.25 km^2 to the mean squared error, then the determination of the mean squared error becomes less precise as the size of the total mean squared error approaches the noise contribution, i.e., a mean squared error on the order of 0.25 km^2. This conclusion has, in fact, been further substantiated by the observed improvement of the procedure with increased ray tracing accuracy, although this improvement has been at the expense of increased computer time usage.

The simultaneous adjustment of many variable

components in $\vec{\xi}$ has been less successful. The increased complexity of the mean squared error hypersurface as the dimensionality of the domain is increased, together with the necessary increase in computer time, would seem to suggest that the simultaneous determination of many variable components is not practical for the present method. However, it should be mentioned that the same difficulties are inherent in most minimization methods. A related issue of the nonuniqueness of $\vec{\xi}$ as obtained from this procedure has not been discussed. This problem is, however, addressed by the methods of *Chuang and Yeh* [1977].

The present procedure has been very effective in the analysis of simulated backscatter leading edges when only a few components of $\vec{\xi}$ have been specified as variables and could probably be made even more efficient through the use of a more sophisticated ray tracing technique.

Acknowledgment. The work described in this paper was supported by the Rome Air Development Center, Deputy for Electronic Technology.

REFERENCES

Backus, G. E., and J. F. Gilbert (1967), Numerical application of a formalism for geophysical inverse problems, *Geophys. J., 13,* 247–276.

Chuang, S. L., and K. C. Yeh (1977), A method for inverting oblique sounding data in the ionosphere, *Radio Sci., 12,* 135–140.

Croft, T. A. (1972), Sky-wave backscatter: A means for observing our environment at great distances, *Rev. Geophys. Space Phys., 10,* 73–156.

Haselegrove, J. (1957), Oblique ray paths in the ionosphere, *Proc. Phys. Soc. London Sect. B, 70,* 653–662.

Hatfield, V. E. (1970), Derivation of ionospheric parameters from backscatter data, in *Ionospheric Forecasting,* edited by V. Agy, *AGARD Conf. Proc., 49,* 16-1–16-9.

Phillips, G. M., and P. J. Taylor (1973), *Theory and Application of Numerical Analysis,* pp. 276–335, Academic, New York.

Rao, N. N. (1974), Inversion of sweep frequency sky wave backscatter leading edge for quasi-parabolic ionosphere layer parameters, *Radio Sci., 9,* 845–847.

Rao, N. N. (1975), Analysis of discrete oblique ionogram traces in sweep frequency sky wave high-resolution backscatter, *Radio Sci., 10,* 149–153.

Yeh, K. C., and C. H. Liu (1972), *Theory of Ionospheric Waves,* pp. 223–307, Academic, New York.